Double Series Resonant DC-DC Converter with Uniform Voltage Stress on High Voltage Transformers

Nor Azura, Samsudin*, Soib, Taib and Shahid, Iqbal

School of Electrical and Electronic Engineering, Engineering Campus, Universiti Sains Malaysia, 14300 Nibong Tebal, Penang, Malaysia

ABSTRACT

This paper proposes a novel double series resonant dc-dc converter with uniform voltage stress on a transformer. It consists of a half-bridge inverter with two power switches (IGBTs), two series resonant tank, two high-voltage transformers and a symmetrical voltage multiplier circuit. A symmetrical voltage multiplier circuit is connected at the secondary side of the high voltage transformer to generate desired high voltage dc output. Due to use of voltage multiplier circuit, the proposed converter requires smaller turns ratio of the high voltage transformer, leading to reduction in size and volume of the transformer. The proposed converter operates in discontinuous current mode by varying the switching frequency of the converter. In a discontinuous current mode operation, all the power switches and output diodes of the rectifier circuit turn-on and turn-off under zero current switching conditions. Therefore, it has features of low switching losses and possibility of light-load operation. Besides, it costs less and is smaller in size compared with conventional double series resonant dc-dc converter. It also has a simple operating principle and suitable for high voltage and high power applications. Experimental results confirm the proposed converter performs better than the others.

Keywords: Series resonant converter, zero current switching, high voltage, dc-dc converter

INTRODUCTION

High voltage dc power supplies are used in electrostatic precipitators, particle accelerators, lasers, X-ray systems and industrial test equipment (Kulkarni et al., 2000). A dc high voltage power supply normally consists of a dc-ac inverter, high voltage transformer (HVT), high voltage rectifier and controller, among others. (Jang et al., 2010). The HVT is the most critical

component in high voltage power supplies. The design of the HVT is quite different compare with the conventional transformer. When HVT is used to produce high output voltage, it has a high number of turn's ratio. Due to this reason, the parasitic capacitance referred to the primary side of the transformer is multiplied by the square of two of the number of the turn's ratio. Therefore, a HVT has significant leakage inductance and parasitic capacitance. The parasitic components give voltage and current spikes and affect the performance of the converter (Li et al., 2007).

To overcome the problems causes by HVT, studies have proposed several types of resonant converters. Resonant converters can achieve zero current switching (ZCS) and zero voltage switching (ZVS) at the converter and can operate at a higher switching frequency that can also reduce the size of the converters (Ye et al., 2008). There are various types of the resonant converter topologies such as series resonant converters (SRC), parallel resonant converters (PRC) and series-parallel resonant converters (SPRC). All of these converters have their own merits and demerits. The SRC is often used in the high voltage power supplies because it is free from saturation and has simple frequency control (Pijl et al., 2009), good efficiency both at heavy and light load (Pan et al., 2013) and inherent capability of short circuit protection (Chakraborty et al., 2002). The SRC that operates in a discontinuous current mode (DCM) are mainly used in high voltage application because of advantages when adopting DCM operation which is ZCS turn-on and anti-parallel diodes turn-on and turn-off naturally at the power switches and low switching losses (Singh et al., 2013). Sze Sing et al., (2012) proposed double series resonant high voltage dc-dc converter in order to reduce the conduction loss and improve efficiency. However, this converter has certain drawbacks, namely unequal dc voltage stress on transformers. It is equal to $V_o/2$ for transformer T_1 while it is zero for transformer T_2. Due to this reason, transformer T_1 need to be designed with larger isolation distance between primary and secondary windings leading to larger leakage inductance compared with transformer T_2.

This paper proposes double series resonant dc-dc converter with uniform voltage stress on HVT-based symmetrical voltage multiplier (SVM). In the proposed converter, the secondary windings of the high voltage transformer are connected to the SVM circuit; therefore, the dc voltage stress on the HVTs is uniform. It is equal for both transformers, T_1 and T_2, respectively because of their common grounding. Therefore, transformer T_1 and T_2 can be designed with same isolation distance between primary and secondary windings so that the value of leakage inductance is same for both transformers, T_1 and T_2. Furthermore, the proposed converters perform better.

CIRCUIT DESCRIPTION AND PRINCIPLE OF OPERATION

The proposed double series resonant dc-dc converter with uniform voltage stress on high voltage transformers is shown in Figure1. The proposed converter circuit consists of half bridge inverter that has two power switches, S_1 and S_2, two resonant capacitors, C_{r1} and C_{r2}, two high voltage transformers, T_1 and T_2, SVM circuit and output load resistor. The leakage inductances, L_{r1} and L_{r2}, are of the primary windings, T_1 and T_2 of the HVTs respectively. The inverter circuit is to invert the lower dc voltage from the input voltage into ac voltage. Power switches S_1 and S_2 operate in complementary fashion with interleaved half switching cycle. The

resonant capacitors, C_{r1} and C_{r2} are connected in series with the leakage inductances, L_{r1} and Lr2 respectively. Therefore, two series resonant tank circuits are formed which are resonant tank circuit-1 and resonant tank circuit-2. Resonant tank circuit-1 consists of L_{r1} and C_{r1}, and resonant tank circuit-2 consists of L_{r2} and C_{r2}. The main purpose of the HVTs is to boost the secondary voltage to desired levels and also to obtain the electrical isolation between primary and secondary side of the HVT circuit. The secondary windings of the transformer are connected to the *m*-stage of the SVM circuit. The secondary voltage of the HVTs is multiplied by *m*-stage; therefore, maximum output voltage of the SVM circuit is nearly $V_o=2mvs_{(max)}$.
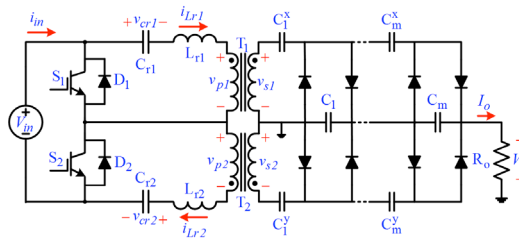

Figure 1. The proposed double series resonant dc-dc converters with uniform voltage stress on high voltage transformers

These series resonant circuits are fed alternatively by operating the power switches with an interleaved half switching cycle. The discontinuous conduction mode (DCM) of operation occurs when the switching frequency, f_s of the converter is less than half of its resonant frequency, f_r, i.e.

$$f_s \le \frac{1}{2} f_r \tag{1}$$

where, f_r is the natural frequency of resonant tank and expressed as

$$f_r = \text{resonant frequency} = \frac{1}{2\pi\sqrt{L_r C_r}} \tag{2}$$

Here, L_r is the leakage inductance and C_r is the resonant capacitor. In the proposed converter, the two resonant capacitors are connected in series to the input dc source through primary windings, so that the voltage stress on these capacitors is reduced to half compared with conventional full-bridge inverter high-voltage dc-dc converter.

ANALYSIS OF STEADY-STATE OPERATION

The key steady-state waveforms of the proposed converter for one complete switching cycle are shown in Figure 2. There are six modes of operation in one switching cycle and the equivalent circuits of these modes of operation are shown in Figure 3. To simplify the analysis, following assumptions are made:

- All the components are assumed to be identical by $L_r = L_{r1} = L_{r2}$ and $C_r = C_{r1} = C_{r2}$.
- The turns ratio of the transformer is $k = N_{P1}/N_{S1} = N_{P2}/N_{S2}$ of the transformers, T_1 and T_2 respectively.

The output voltage in the primary side of the transformer is obtained by dividing secondary voltage with transformer turn's ratio, k and it is assumed that capacitors of the voltage multiplier circuit are large enough so that voltage ripples across these capacitors are significant in a steady-state operation.
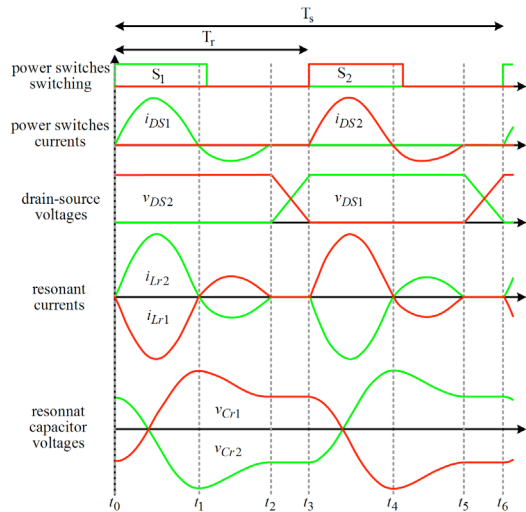

Figure 2. The key steady-state waveform of the proposed resonant converters over one switching cycle

Mode 1 [t0 ≤ t ≤ t1]: This mode begins when the power switch, S_1 is turned on and the resonant currents, i_{Lr1} and i_{Lr2} start flowing sinusiodally in the negative and positive directions respectively. Hence, resonant capacitor C_{r1} is discharging and capacitor C_{r2} is charging during this mode of the operation. The resonant currents increases from zero, thus S_1 are turn-on with ZCS and dc source supplies power to be consumed by the load and stored in the resonant tank. Input current i_{in} is identical to the i_{Lr2} in this mode. This mode ends when the i_{Lr1} and i_{Lr2} becomes zero at time $t = t_1$. The equivalent circuit for this mode is illustrated in Figure 3(a). The equations of $iL_{r1(t)}, v_{Cr1(t)}, i_{Lr2(t)},$ and $v_{Cr2(t)}$ during this mode are given by

$$i_{Lr1}(t) = \frac{-\dfrac{V_{in}}{2} - \dfrac{V_o}{4k}}{Z_r} \sin \omega_r t \tag{3}$$

$$v_{Cr1}(t) = \left(-\frac{V_{in}}{2} - \frac{V_o}{4k}\right)(1 - cos\,\omega_r t) + \frac{V_{in}}{2} + \frac{V_o}{2k} \tag{4}$$

$$i_{Lr2}(t) = \frac{\frac{V_{in}}{2} + \frac{V_o}{4k}}{Z_r} sin\,\omega_r t \tag{5}$$

$$v_{Cr2}(t) = \left(\frac{V_{in}}{2} + \frac{V_o}{4k}\right)(1 - cos\,\omega_r t) + \frac{V_{in}}{2} - \frac{V_o}{2k} \tag{6}$$

where $\omega_r = \dfrac{1}{\sqrt{L_r C_r}}$, $Z_r = \sqrt{\dfrac{L_r}{C_r}}$, $L_r = L_{r1} = L_{r2}$, $C_r = C_{r1} = C_{r2}$ and $k = \dfrac{N_{S1}}{N_{P1}} = \dfrac{N_{S2}}{N_{P2}}$

Mode 2 [t$_1$ ≤ t ≤ t$_2$]: At the beginning of this mode at time $t=t_1$, resonant currents, i_{Lr1} and i_{Lr2} start flowing though the anti-parallel diode, D_1, of the power switch, S_1. During this mode, the i_{Lr1} and i_{Lr2} swings sinusoidally in the positive and negative directions respectively. Therefore, S_1 is turn off with ZCS and ZVS conditions. This mode ends when the i_{Lr1} and i_{Lr2} reach zero at $t=t_2$. The equivalent circuit related to this mode of operation is shown in Figure 3(b). The equations of $i_{Lr1}(t)$, $v_{Cr1}(t)$, $i_{Lr2}(t)$ and $v_{Cr2}(t)$ during this mode are given by

$$i_{Lr1}(t) = \frac{\frac{V_{in}}{2} - \frac{V_o}{4k}}{Z_r} sin\,\omega_r\left(t - \frac{\pi}{\omega_r}\right) \tag{7}$$

$$v_{Cr1}(t) = \left(\frac{V_{in}}{2} - \frac{V_o}{4k}\right)\left(1 - cos\,\omega_r\left(t - \frac{\pi}{\omega_r}\right)\right) - \frac{V_{in}}{2} \tag{8}$$

$$i_{Lr2}(t) = \frac{-\frac{V_{in}}{2} + \frac{V_o}{4k}}{Z_r} sin\,\omega_r\left(t - \frac{\pi}{\omega_r}\right) \tag{9}$$

$$v_{Cr2}(t) = \left(-\frac{V_{in}}{2} + \frac{V_o}{4k}\right)\left(1 - cos\,\omega_r\left(t - \frac{\pi}{\omega_r}\right)\right) + \frac{3V_{in}}{2} \tag{10}$$

Mode 3 [t$_1$ ≤ t ≤ t$_2$]: At time $t=t_2$, the power switch, S_1 are turn-off and the resonant currents, i_{Lr1} and i_{Lr2} are zero. As a result, the voltages across resonant capacitors v_{Cr1} and v_{Cr2} will be same as at time $t=t_2$. The minimum duration of this mode must be greater than zero to ensure DCM operation of the converter. Therefore, no energy transfer occurs from source to load during this mode. The equivalent circuit related to this mode of operation is shown in Figure 3(c). The equations of $v_{Cr1}(t)$ and $v_{Cr2}(t)$ during this mode are given by

$$v_{Cr1}(t) = \frac{V_{in}}{2} - \frac{V_o}{2k} \tag{11}$$

$$v_{Cr2}(t) = \frac{V_{in}}{2} + \frac{V_o}{2k} \tag{12}$$

Mode 4 [$t_2 \leq t \leq t_3$]: This mode begins at time $t=t_3$ when the resonant currents, i_{Lr1} and i_{Lr2} begin to flow through the power switch, S_2. The i_{Lr1} is swings sinusoidally in the positive direction and the i_{Lr2} in the opposite direction. Therefore, the energy stored in the L_{r2} and C_{r2} during mode is transferred to the load. This mode ends when the i_{Lr1} and i_{Lr2} becomes zero at time $t=t_4$. The equivalent circuit for this mode is illustrated in Figure 3(d). The equations of $i_{Lr1}(t)$, $v_{Cr1}(t)$, $i_{Lr2}(t)$, and $v_{Cr2}(t)$ during this mode are given by

$$i_{Lr1}(t) = \frac{\frac{V_{in}}{2} + \frac{V_o}{4k}}{Z_r} \sin \omega_r \left(t - \frac{T_s}{2} \right) \tag{13}$$

$$v_{Cr1}(t) = \left(\frac{V_{in}}{2} + \frac{V_o}{4k} \right) \left(1 - \cos \omega_r \left(t - \frac{T_s}{2} \right) \right) + \frac{V_{in}}{2} - \frac{V_o}{2k} \tag{14}$$

$$i_{Lr2}(t) = \frac{-\frac{V_{in}}{2} - \frac{V_o}{4k}}{Z_r} \sin \omega_r \left(t - \frac{T_s}{2} \right) \tag{15}$$

$$v_{Cr2}(t) = \left(-\frac{V_{in}}{2} - \frac{V_o}{4k} \right) \left(1 - \cos \omega_{r2} \left(t - \frac{T_s}{2} \right) \right) + \frac{V_{in}}{2} + \frac{V_o}{2k} \tag{16}$$

Mode 5 [$t_3 \leq t \leq t_4$]: At time $t=t_4$ when the resonant currents, i_{Lr1} and i_{Lr2} begin flowing through anti-parallel diode, D_2, of the power switch, S_2, in the reverse direction. In this mode, S_2 is turn-off under ZCS and ZVS conditions. In this mode, both resonant tanks transfer energy to the load. This mode ends when the i_{Lr1} and i_{Lr2} becomes zero at time $t=t_5$. The equivalent circuit related to this mode of operation is shown in Figure 3(e). The equations of $i_{Lr1}(t)$, $v_{Cr1}(t)$, $i_{Lr2}(t)$, and $v_{Cr2}(t)$ during this mode are given by

$$i_{Lr1}(t) = \frac{-\frac{V_{in}}{2} + \frac{V_o}{4k}}{Z_r} \sin \omega_r \left(t - \frac{\pi}{\omega_r} - \frac{T_s}{2} \right) \tag{17}$$

$$v_{Cr1}(t) = \left(-\frac{V_{in}}{2} + \frac{V_o}{4k} \right) \left(1 - \cos \omega_r \left(t - \frac{\pi}{\omega_r} - \frac{T_s}{2} \right) \right) + \frac{3V_{in}}{2} \tag{18}$$

$$i_{Lr2}(t) = \frac{\frac{V_{in}}{2} - \frac{V_o}{4k}}{Z_r} \sin \omega_r \left(t - \frac{\pi}{\omega_r} - \frac{T_s}{2} \right) \tag{19}$$

$$v_{Cr2}(t) = \left(\frac{V_{in}}{2} - \frac{V_o}{4k} \right) \left(1 - \cos \omega_r \left(t - \frac{\pi}{\omega_r} - \frac{T_s}{2} \right) \right) - \frac{V_{in}}{2} \tag{20}$$

Mode 6 [$t_4 \leq t \leq t_5$]: This mode is same with Mode 3, so the power switch, S_2 is turn-off and the resonant currents i_{Lr1} and i_{Lr2} are zero. As a result, the voltages across resonant capacitors v_{Cr1} and v_{Cr2} will be constant as at time $t=t_5$. The equivalent circuit is shown in Figure 3(f) and equations of $v_{Cr1}(t)$ and $v_{Cr2}(t)$ are given by

$$v_{Cr1}\left(t\right) = \frac{V_{in}}{2} + \frac{V_o}{2k} \tag{21}$$

$$v_{Cr2}\left(t\right) = \frac{V_{in}}{2} - \frac{V_o}{2k} \tag{22}$$
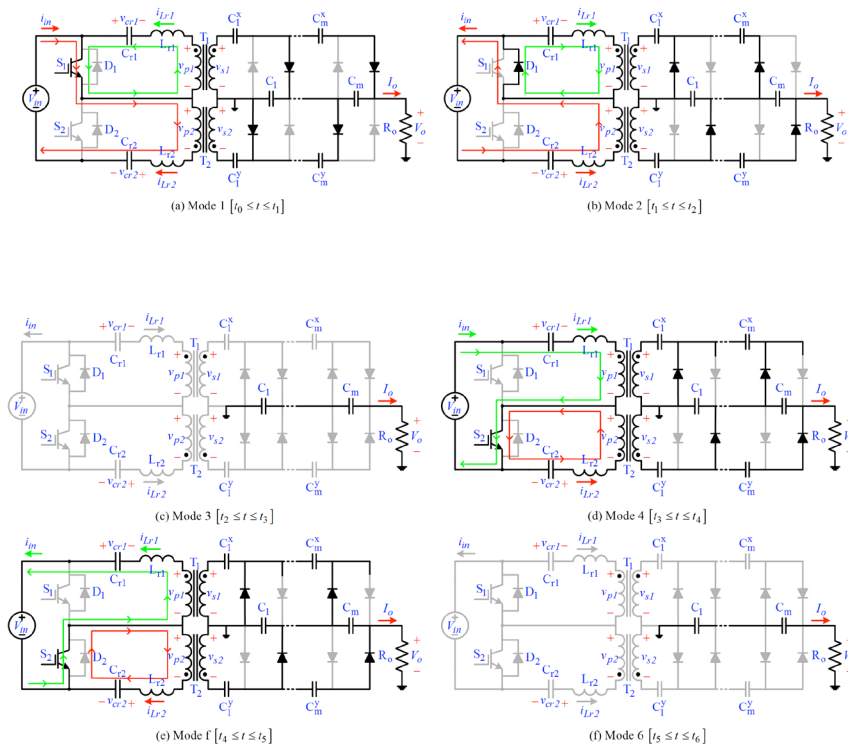

Figure 3. The equivalent circuit of the proposed resonant converter for each operation modes

RESULTS AND DISCUSSIONS

A prototype of the proposed resonant converter was built and tested to validate the feasibility of the converter. The design specifications of the experimental prototype are as follows: $V_{in}=100$ V, $k=5$, $fr=75$ kHz, $R_o=20$ kΩ, $Cr=C_{r1}=C_{r2}=110$ nF, and $L_r=L_{r1}=L_{r2}=46$ µH. Figure 4(a) and 4(b) shows the waveforms of the gate signal of the power switches V_{GE1} and V_{GE2} and resonant currents, i_{Lr1} and i_{Lr2} for switching frequency of 25-kHz and 35-kHz respectively. It can be observed that when the power switch, S_1 is turned on, i_{Lr1} and i_{Lr2} flow sinusoidally in the

negative and positive direction respectively. When power switch S_2 is turned-on, then i_{Lr1} and i_{Lr2} flow in the positive and negative direction respectively. Thus, the both resonant currents are inverted replica of each other. From the waveforms, power switches S_1 and S_2 are turned ON and OFF at ZCS. Thus, the switching losses are negligible.
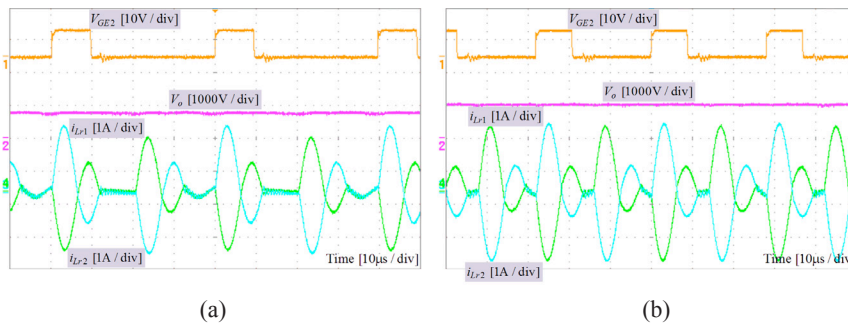

(a)   (b)

Figure 4. Experimental waveforms of the gate signal of the power switches, V_{GE1} and V_{GE2} and resonant currents, i_{Lr1} and i_{Lr2} for switching frequency (a) 25-kHz and (b) 35-kHz respectively

Figures 5(a) and 5(b) show the waveforms of the gate signal at the power switch, output voltage, V_o and resonant currents for switching frequency of 25-kHz and 35-kHz respectively. The output voltage and the amplitude of resonant currents are at the switching frequency of 25-kHz is 772-V and 3.5-A respectively. At the switching frequency 35-kHz, the output voltage and resonant currents is 1020-V and 4.2-A respectively. For a fixed value load resistance, the output voltage and resonant currents are increased when increasing the switching frequency
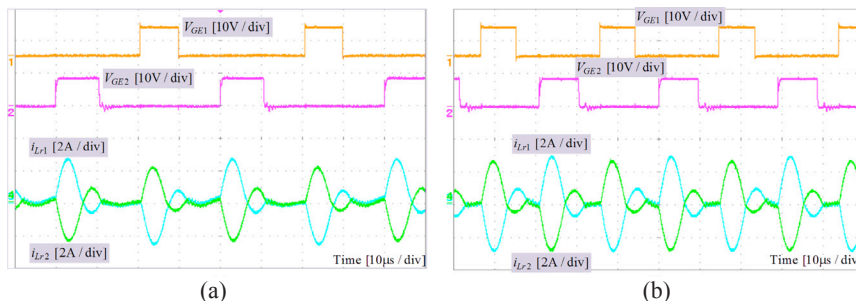

(a)   (b)

Figure 5. Experimental waveforms of the gate signal of the power switch, output voltage, V_o and resonant currents, i_{Lr1} and i_{Lr2} for switching frequency (a) 25-kHz and (b) 35-kHz respectively

Figures 6(a) and 6(b) shows the waveform of the resonant voltages, V_{Cr1} and V_{Cr2} and the resonant currents for the switching frequency of 25-kHz and 35-kHz respectively. It can be observed that resonant capacitors, C_{r1} and C_{r2} discharge and charge respectively when the power switches, S_1 is turned on. Similarly, when the power switches, S_2 is turned on, C_{r1} and C_{r2} charge and discharge respectively. The peak-to-peak voltages swing of the resonant

capacitors at the Figure 6(a) is smaller compared with Figure 6(b) because of the low switching frequency. Besides, the average resonant voltage C_{r1} and C_{r2} is equal to the $V_{in}/2$ as shown in Figures 6(a) and 6(b).
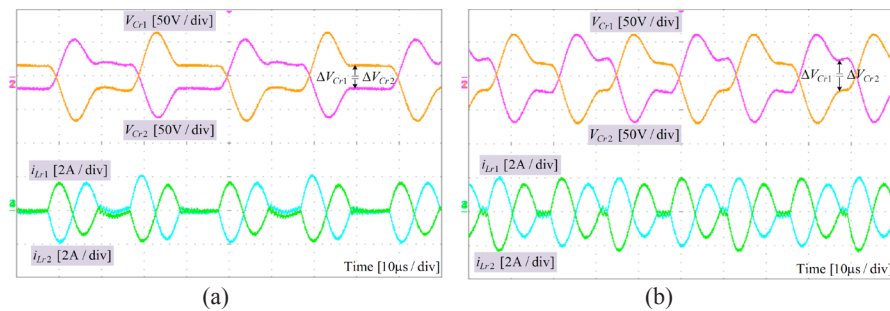

Figure 6. Experimental waveforms of the resonant voltages, V_{Cr1} and V^{Cr2} and resonant currents, i_{Lr1} and i_{Lr2} for switching frequency (a) 25-kHz and (b) 35-kHz respectively

CONCLUSION

A double series resonant dc-dc converter with uniform voltage stress on high voltage transformers suitable for high output voltage applications has been proposed in this paper. Symmetrical voltage multiplier (SVM) is used to convert ac output voltage/current at the secondary transformer to dc ones. The SVM facilitates the decrease in the diode ratings, isolation requirement, and transformer turns ratio, as well as facilitates an increase in the total output filter capacitance. The input voltage of 100-V boosts up to 1020-V for switching frequency, 35-kHz with the resonant currents which is 4.2-A in this proposed converter. The proposed converter has shown lower switching losses because the power switches and output diodes operate with ZCS condition under DCM operation.

ACKNOWLEDGEMENT

REFERENCES

Chakraborty, C., Ishida, M., & Hori, Y. (2002). Novel half-bridge resonant converter topology realized by adjusting transformer parameters. *Journal of IEEE Transactions on Industrial Electronics, 49*(1), 197-205.

Jang, S. R., Ryoo, H. J., Kim, J. S., & Ahn, S. H. (2010). Design and analysis of series resonant converter for 30kW industrial magnetron. In *Proceedings of Conference on Industrial Electronics Society* (p.415-420). IEEE.

Kulkarni, R. D., Bisht, D. S., Bhaumik, P. K., Vyas, H. P., & Sinha, R. K. (2000). High current regulated, variable DC power supplies for simulating power transients expected in nuclear reactors. In *Proceedings of International Conference on Industrial Technology* (p.530-535). IEEE.

Li, J., Niu, Z., Zhang, Z., & Zhou, D. (2007). Analysis of Resonant Converter with Multiplier. In *Proceedings of Conference on Industrial Electronics and Applications* (p.326-331). IEEE.

Pan, S., Pahlevaninezhad, M., & Jain, P. K. (2013). Adaptive hybrid primary/secondary-side digital control for series resonant DC-DC converters in 48V VR applications. In *Proceedings of Conference on Energy Conversion Congress and Exposition* (p.4920-4925). IEEE.

Pijl, F. F. A. V. d., Castilla, M., & Bauer, P. (2009). Implementation of an adaptive sliding-mode control for a quantum series-resonant converter. In *Conference on Power Electronics and Applications* (p.1-10). IEEE.

Singh, Y. V., Viswanathan, K., Naik, R., Sabate, J. A., & Lai, R. (2013). Analysis and control of phase-shifted series resonant converter operating in discontinuous mode. In *Proceedings of Conference on Applied Power Electronics and Exposition* (p.530-535). IEEE.

Sze Sing, L., Iqbal, S., & Jamil, M. K. M. (2012). A novel ZCS-SR voltage multiplier based high-voltage DC power supply. In *Proceedings of International Conference on Circuits and Systems* (p.2092-2097). IEEE.

Ye, Z., & Zhixiang, L. (2008). Modeling and design of a pulse phase modulated resonant inverter system. In *Proceedings of International Conference on Telecommunications Energy* (p.1-7). IEEE.